remote sensing

MDPI

Article

Comparison of Forest Restorations with Different Burning Severities Using Various Restoration Methods at Tuqiang Forestry Bureau of Greater Hinggan Mountains

Guangshuai Zhao [1], Erqi Xu [2], Xutong Yi [1,*], Ye Guo [1] and Kun Zhang [1]

[1] Development Research Center, National Forestry and Grassland Administration, Beijing 100714, China; zhaogs.10s@igsnrr.ac.cn (G.Z.)

[2] Key Laboratory of Land Surface Pattern and Simulation, Institute of Geographic Sciences and Natural Resources Research, Chinese Academy of Science, Beijing 100101, China

* Correspondence: yixutong@gmail.com; Tel.: +86-010-84239170

Abstract: Forest disturbances and restoration are key processes in carbon transmission between the terrestrial surface and the atmosphere. In boreal forests, fire is the most common and main disturbance. The reconstruction process for post-disaster vegetation plays an essential role in the restoration of a forest's structure and function, and it also maintains the ecosystem's health and stability. Remote sensing monitoring could reflect dynamic post-fire features of vegetation. However, there are still major differences in the remote sensing index in terms of regional feasibility and sensibility. In this study, the largest boreal primary coniferous forest area in China, the Greater Hinggan Mountains forest area, was chosen as the sampling area. Based on time series data from Landsat-5 TM surface reflectance (SR) and data obtained from sample plots, the burned area was extracted using the Normalized Burn Ratio (*NBR*). We used the pre- and post-fire difference values (*dNBR*) and compared them with survey data to classify the burn severity level. The Normalized Difference Vegetation Index (NDVI) (based on spectrum combination) and the Disturbance Index (DI) (based on Tasseled-Cap transformation) were chosen to analyze the difference in the degree of burn severity and vegetation restoration observed using various methods according to the sequential variation feature from 1986 to 2011. The results are as follows: (1) The two remote sensing indexes are both sensitive to fire and the burn severity level. When a fire occurred, the NDVI value for that year decreased dramatically while the DI value increased sharply. Alongside these findings, we observed that the rangeability and restoration period of the two indexes is significantly positively correlated with the degree of burn severity. (2) According to these two indexes, natural vegetation restoration was faster than the restoration achieved using artificial methods. However, compared with the NDVI, the DI showed a clearer improvement in restoration, as the restoration period the DI could evaluate was longer in two different ways: the NDVI illustrated great changes in the burn severity in the 5 years post-fire, while the DI was able to show the changes for more than 20 years. Additionally, from the DI, one could identify felling activities carried out when the artificial restoration methods were initially applied. (3) From the sample-plot data, there were few differences in forest canopy density—the average was between 0.55 and 0.6—between the diverse severity levels and restoration methods after 33 years of recovery. The average diameter at breast height (DBH) and height values of trees in naturally restored areas decreased with the increase in burn severity, but the values were obviously higher than those in artificially restored areas. This indicates that both the burn severity level and restoration methods have important effects on forest restoration, but the results may also have been affected by other factors.

Keywords: forest fire; forest restoration; remote sensing index; Landsat-5 data; burning severity; restoration methods

check for updates

Citation: Zhao, G.; Xu, E.; Yi, X.; Guo, Y.; Zhang, K. Comparison of Forest Restorations with Different Burning Severities Using Various Restoration Methods at Tuqiang Forestry Bureau of Greater Hinggan Mountains. *Remote Sens.* **2023**, *15*, 2683. https://doi.org/10.3390/rs15102683

Academic Editors: Eric Ariel L. Salas, Kenneth G. Boykin and Hubert Hasenauer

Received: 21 March 2023
Revised: 2 May 2023
Accepted: 19 May 2023
Published: 22 May 2023

1. Introduction

The monitoring of forest disturbances has significance in global carbon cycle research and in the study of policies. It is also an important factor in the identification of spatial and temporal changes in forest management [1,2]. Fire is the most common forest disturbance and is one factor that leads to reductions in forest carbon stock [3]. In recent years, alongside global warming and the increasing prevalence of extreme weather events, the risk level of forest fires has been rising [4–6]. Forest fires have taken place all over the world, such as severe forest fires in California, US; Australia; and Liangshan County, Sichuan, China. These disasters have a serious impact on the function of the carbon cycle and carbon storage of ecosystems as well as on human life and property [7,8]. Therefore, forest fires have attracted attention from governments and academic circles worldwide. To maintain and enhance ecosystem services, it is very important to monitor and assess forest fire disturbance, especially through the continuous monitoring of post-fire vegetation restoration processes and the scientific assessment of forest recovery conditions after super-large fires. On the one hand, the accuracy of forest carbon sink estimation and prediction can be improved [9]. On the other hand, the study basis of scientific support for forest protection and management, as well as the simulation of vegetation growth, will be strengthened.

In traditional forest fire monitoring and assessment methods, forest field investigations are most commonly adopted, which is largely limited by time and economic efficiency. Additionally, it is difficult to carry out large-scale manual surveys, and the spatial heterogeneity problem in forest ecosystems is difficult to solve effectively [10,11]. The development of satellite remote sensing technology provides data sources and technical support for the monitoring of large-scale areas and continuous forest disturbances [12,13].

Compared with traditional ground monitoring, remote sensing images have the advantages of shorter imaging periods, wider monitoring ranges, and more sensitivity to forest disturbances [14,15]. Landsat data have the most potential in monitoring burned areas and vegetation dynamics [16]. On the one hand, Landsat data have higher spatial resolutions than NOAA or MODIS data, which makes them suitable for the study of forest disturbances and their influence on forest carbon flux at the regional level [17]. On the other hand, compared with the new generation of high-resolution satellite data and noctilucent remote sensing satellite data, Landsat series data have a longer time span, especially Landsat-5 TM, which provides long-term and high-quality operation to enable data support for the continuous monitoring of the Earth's surface.

At present, there are two analysis methods used to monitor forest fire disturbances, one of which is based on a simple spectral combination, and the other is based on Tasseled-Cap transformation [1,18,19]. The Normalized Difference Vegetation Index (NDVI) is the most commonly used forest disturbance monitoring method, which is based on a spectral combination. The NDVI is sensitive to vegetation activity, density, and effective photosynthetic radiation absorbed by vegetation [20,21]. However, it is easily disturbed by soil background, and it is less sensitive to dense forest cover [22,23]. The Normalized Burn Ratio (*NBR*) is another analytical method based on the spectral combination of forest fire disturbances. Using the *dNBR*—which is the difference value of the *NBR* before and after a fire—the burning area and severity can be extracted effectively [24,25]. The Disturbance Index (DI) is the most widely used forest disturbance monitoring method and is based on the Tasseled-Cap transformation [26–28]. This method has the ability to respond strongly to different types of forest disturbances, especially deforestation, forest pests and diseases, afforestation, and so on [13,29,30].

The Greater Hinggan Mountains forest region, located in the northeast of China, is the largest boreal coniferous forest in China with rich forest resources; however, there is a high risk of forest fires in this area. Vegetation restoration in this region has great carbon sequestration potential. According to research carried out between 2010 and 2016, through vegetation recovery, especially large-scale afforestation in northeast China, the carbon sink capacity of the terrestrial biosphere offset approximately 45% of artificial carbon emissions over the same period [31]. Fire is the main disturbance in boreal forests and has been proven to release large amounts of carbon into the atmosphere via burning [32]. Therefore, monitoring the forest's response to fire and the dynamic recovery process in the Greater Hinggan Mountains can be an effective aspect of climate and carbon system models [33,34]. Most of the previous macro studies on post-fire forest assessment used the NDVI, which could not fully reflect the vegetation changes. In this study, the Disturbance Index (DI) was added. Along with the field survey data, the following vegetation restoration situations will be discussed: (1) the temporal sequence characteristics of vegetation restoration using two remote sensing indices with different fire severities; (2) the temporal sequence characteristics of vegetation restoration using two remote sensing indices with different restoration methods; (3) the comparison of forest restoration results for fires with different severity levels and using different restoration methods. A research basis and scientific support for the strengthening of forest protection and management as well as vegetation reconstruction after a forest fire can be provided by the scientific monitoring and evaluation of post-fire vegetation restoration processes.

2. Methods

2.1. Study Area

The Tuqiang Forestry Bureau is located in Mohe County at the northern foot of the Greater Hinggan Mountains, bordering the Amur Forestry Bureau in the east, the Mangui Forestry Bureau of Inner Mongolia in the south, the Xilinji Forestry Bureau in the west, and faces Russia across Heilongjiang in the north. The geographical coordinates are 122°18′28′′–123°28′10′′E and 52°15′35′′–53°33′42′′N. The major mountain range in this area lies from northeast to southwest. The terrain is long and narrow and is high in the south and low in the north. The region is located in a cold temperate, continental monsoon climate zone, with long, cold winters and short, hot summers. The average annual precipitation is about 400 mm. The frost-free period is 80 to 90 days. The average annual temperature is −3.9 °C. The natural vegetation of this region is of the boreal coniferous type; major conifer species include Dahurian larch (*Larix gmelinii*) and Mongolian scotch pine (*Pinus sylvestris*), which both grow in pure and mixed stands. After a fire disturbance, these species are often replaced by northern hardwoods, including birch (*Betula platyphylla*) and aspen (*Populus davidiana*). On 6 May 1987, a devastating forest fire occurred in this area; large areas of natural forests managed by the Tuqiang Forestry Bureau were destroyed, leading to a substantial decline in forest resources. The burned area covered 2310 km^2, and this accounted for more than 80% of the total forest area [35]. The "5·6 Fire" was the most severe fire since the founding of the People's Republic of China, which destroyed one-fifth of the Greater Hinggan Mountains forest area (a burned area of 1.33×10^4 km^2 and a burned forest area of 1.01×10^4 km^2). More than 50,000 people became homeless as a result of the fire, and hundreds died; in addition, there was a direct economic loss of over CNY 500 million and an indirect economic loss of CNY 6 billion [36,37]. In this article, through the comparison of remote sensing images from 1986 and 1987 by visual interpretation, the post-fire region of the Tuqiang Forestry Bureau was selected as the study area (Figure 1).

2.2. Data Sources

When using remote sensing image features to analyze canopy restoration results, the time period of the images is an important factor that needs to be taken into consideration. If the images were taken in the vigorous growing season, with high density and a large covered canopy, newly planted trees might be interpreted as mature forests. In fact, during a 20- or 30-year post-fire period, trees will still be in their infancy. In this situation, the effect of forest restoration will be difficult to observe, and the differences in the features of the remote sensing images taken of fires of various severity levels and using various restoration measures will be weakened. Therefore, in this study, the initial growing stages of trees were selected to represent their growth condition because when trees are growing well and are older, the remote sensing index is higher, which illustrates the difference in the forest restoration effect. The Landsat-5 TM surface reflectance (SR) remote sensing images used in this study were obtained from the Google Earth Engine (GEE) cloud computing platform. There were two kinds of images: (1) remote sensing images from 1986 to 1987, from June to September, in order to extract data regarding the burned area and burning severity; (2) and remote sensing images from 1986 to 2011, in June or July, in order to extract data regarding the annual vegetation restoration process. The yearly image dates are shown in Table 1. Remote sensing images from 2011 and onwards were not extracted and analyzed because, based on previous studies, after 20 years of recovery in a burned area, it is difficult to observe differences in canopy restoration using the remote sensing index. The QA band generated using the CFMask algorithm was used to mask low-quality pixels such as clouds, snow, and cloud shadow.

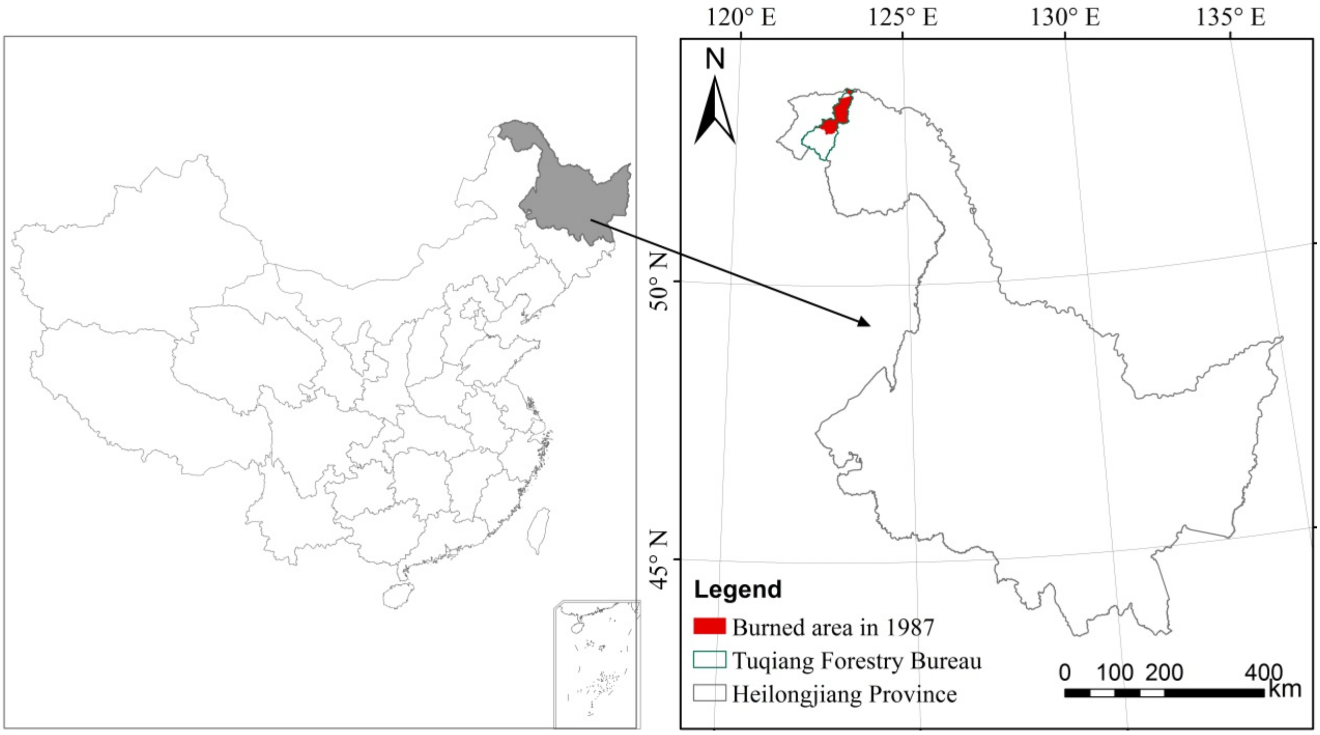

Figure 1. Study area.

Table 1. Acquisition date of Landsat-5 TM images.

Year	1986	1987	1988	1989	1990	1991	1992	1993	1994	1995	1996	1997	1998
Date (Day/Month)	12/6	15/6	17/6	13/6 [1]	16/6 [1]	10/6	12/6	1/7	4/7	23/7	16/7 [2]	26/6	15/7
Year	1999	2000	2001	2002	2003	2004	2005	2006	2007	2008	2009	2010	2011
Date (Day/Month)	16/6	18/6	21/6	24/6	20/6 [1]	29/6	2/7	5/7	11/7 [1]	24/6	27/6	23/6 [1]	3/7

Note: [1] means that Landsat image was utilized by path 121 and row 23; [2] means that Landsat image was utilized by path 123 and row 23; others mean that Landsat image was utilized by path 122 and row 23.

The data sources came from the Tuqiang Forestry Bureau, which mainly included forest resources inventory data, forest stand maps in 1987 and 2020, a map of burn severity in 1987, a management plan, and field survey data. The forest resources inventory data and field survey data were obtained from the second-class inventory database of forest resources in the Greater Hinggan Mountains. To guarantee 95% sampling precision, 1263 forest compartments were investigated by using sample plots with sizes of 0.0667 hm^2. According to the condition and complexity of each compartment, sample plots could be added. The data included the proportion of the area affected by the fire with different burn severities and the measurement data for each tree: the diameter at breast height (DBH), height, and canopy density. The management plan included the area and location data of different restoration methods. In total, 7% and 93% of the burned area were restored by artificial and natural methods, respectively (Figure 2).

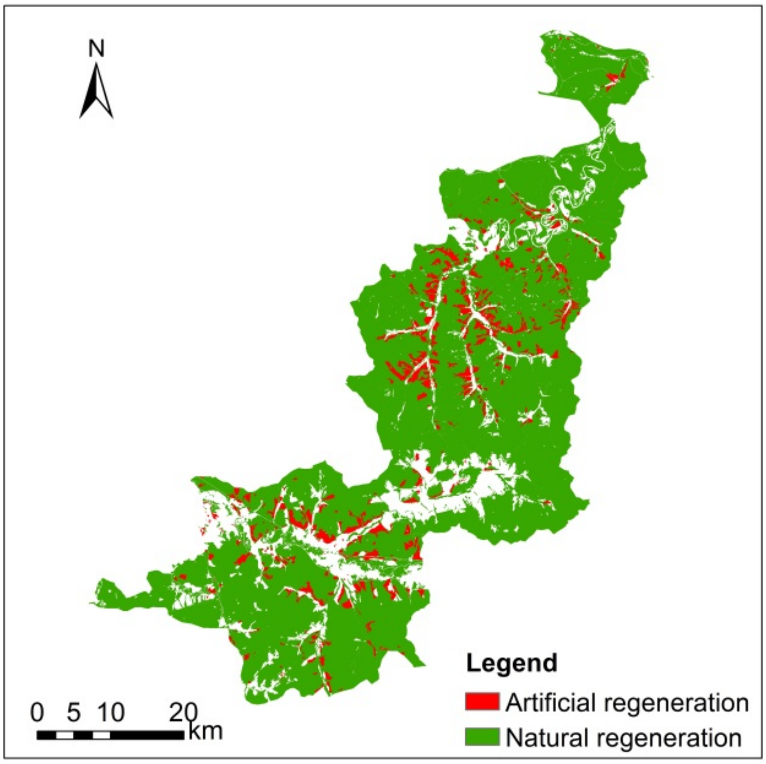

Figure 2. Spatial distribution of different forest restoration methods.

2.3. Calculation Method

2.3.1. Burn Severity Mapping

$$NBR = \frac{NIR - SWIR\,2}{NIR + SWIR\,2} \quad (1)$$

In the formula, NIR is Landsat-5 near-infrared, and $SWIR\,2$ is Landsat-5 shortwave infrared 2.

Based on $dNBR$, the difference value of NBR images between 1986 and 1987, grades of burn severity could be calculated as follows:

$$dNBR = NBR_{1987} - NBR_{1986} \quad (2)$$

Before the assessment, we removed images of non-forest land by screening the map with a non-forest mask ($NBR < 0.5$ in 1986). Based on the $dNBR$ images, a threshold division was set to classify the burning severity as unburned, light burn severity, moderate burn severity, and severe burn severity (Table 2). The $dNBR$ threshold was determined by the burned area ratio from the forest survey in different degrees after the fire in 1987 and by referring to the map of burn severity in 1987 and previous research results [38,39].

Table 2. Burn severity classification standard.

Burned Severity	Trees Consumed by Fire (%)	Area Ratio (%)	*dNBR* Threshold
unburned	No fire	16	≤0.23
lightly burned	≤30	22	0.23–0.60
moderately burned	30–70	15	0.60–0.83
severely burned	≥70	47	≥0.83

2.3.2. NDVI Calculation

$$NDVI = \frac{NIR - RED}{NIR + RED} \quad (3)$$

Among these, *RED* is the Landsat-5 red light band.

2.3.3. DI Calculation

The Forest Disturbance Index (*DI*) was calculated from the brightness, greenness, and humidity after the Tasseled-Cap transformation. The higher the *DI*, the greater the disturbance of the forest ecosystem. The formula is as follows:

$$DI = B_n - (G_n + W_n) \quad (4)$$

Among which,

$$B_n = \left(B - B_\mu\right)/B_\sigma \quad (5)$$

$$G_n = \left(G - G_\mu\right)/G_\sigma \quad (6)$$

$$W_n = \left(W - W_\mu\right)/W_\sigma \quad (7)$$

In the formula, B_n, G_n, and W_n represent Tasseled-Cap brightness, greenness, and wetness after normalization using pure forest pixels. B_μ, G_μ, and W_μ and B_σ, G_σ, and W_σ are the mean and standard deviation of B_n, G_n, and W_n in the pure forest area, respectively. The pure forest pixels were extracted automatically from the cumulative frequency histogram extraction algorithm of the *NDVI* (>90%) [40]. In addition, Tasseled-Cap transformation was calculated by the method devised by Crist (1985), which is based on the use of surface reflectance to carry out Tasseled-Cap transformation matrix calculation [41].

2.3.4. NDVI and DI Time Series Analysis

The NDVI and DI time series values in all the scenes were calculated. Before the calculation, we removed non-forest areas using the above-mentioned method. Then, the average NDVI and DI values of the "burned forest" under various burned severities and restoration methods and "unburned forest" areas were calculated (by Esri ArcGIS 10) and developed to become time series. Trend analysis and analysis of variance (ANOVA) were used (by IBM SPSS Statistics 24) to quantify the different groups' NDVI and DI values in three different time periods (1986–2011, 1987–1992, and 1993–2011) [37]. When data were not available for some levels, the least significant difference (LSD) method was used for multiple comparisons.

3. Results

3.1. Comparison of Forest Remote Sensing Index with Different Burn Severities

According to the forest recovery situation in 2011, 99% of the study area's NDVI was larger than 0.7 (Figure 3a), with an average value of 0.83 ± 0.04, while the DI value was smaller than 9 (Figure 3b), with an average value of 1.36 ± 2.35. After about 20 years of growth after the fire in the study area, it was difficult to observe the differences in canopy recovery from the two forest remote sensing indexes.

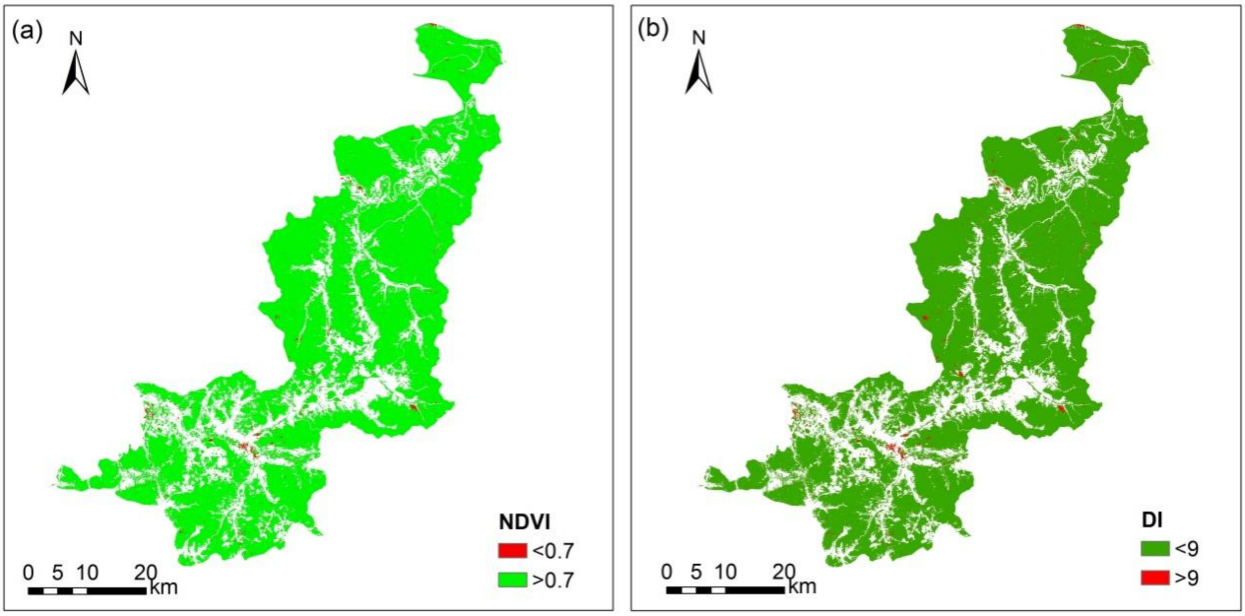

Figure 3. Spatial distribution of vegetation index: (**a**) NDVI (Normalized Difference Vegetation Index); (**b**) DI (Disturbance index) in 2011.

According to the difference value of the *NBR* between 1987 and 1986 images, the *dNBR* was between −0.67 and 1.52 (Figure 4a), and the average value was 0.69 ± 0.36. The burn severity was classified by the *dNBR*. The results showed that 62% of the study area was moderately burned or severely burned (Figure 4b), which demonstrated that the study area was heavily destroyed by fire.

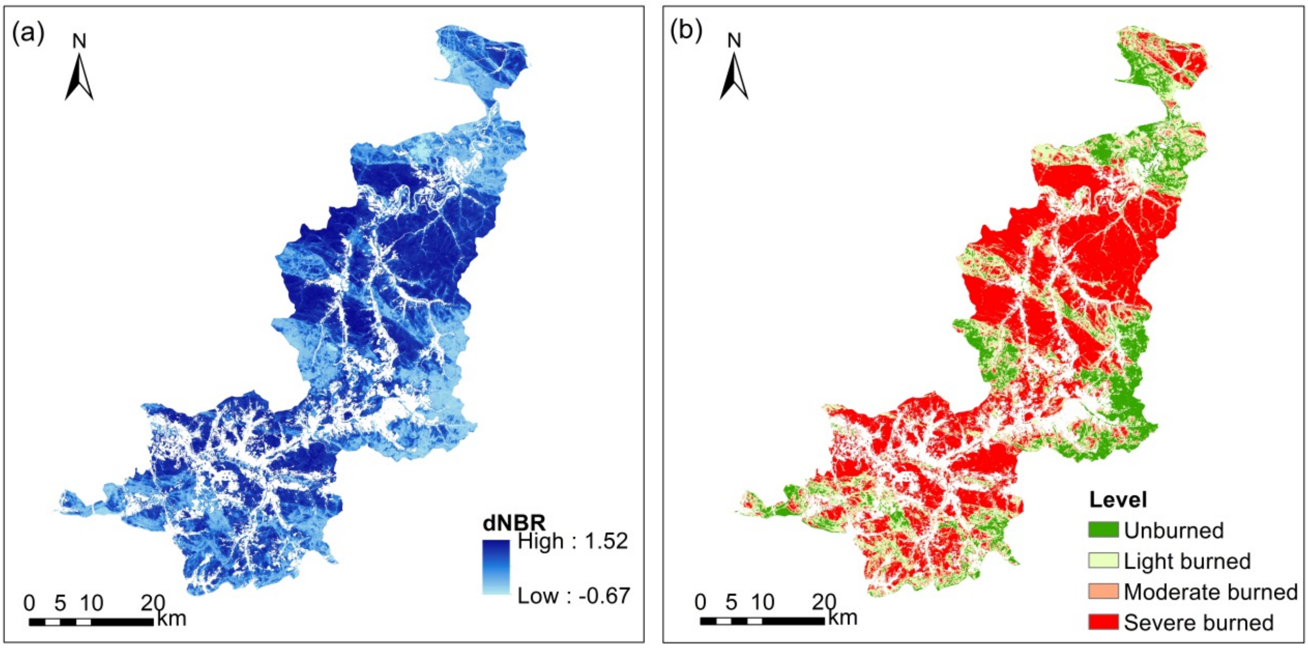

Figure 4. Burn severity mapping: (**a**) *dNBR* values; (**b**) different burn severities.

We wanted to analyze further the change trends of the NDVI and DI regarding different burn severities (Figure 5). In 1987 and the following 5 years, the NDVI displayed significant differences in burn severities (F = 3.16, p < 0.05); however, the vegetation recovered quickly after the fire, and there were hardly any differences with the vegetation in 1993–2011 (F = 0.71, p = 0.55) (Figure 5a). Compared with the NDVI in 1986–2011 (F = 2.03, p = 0.12), the DI showed more significant differences in burn severities ($F = 18.06$, $p < 0.001$). The higher the DI value, the higher the burn severity. It took about 20 years for the DI to be on the same level. The DI showed a significant difference in burn severity during 1993–2011 ($F = 12.74$, $p < 0.001$) (Figure 5b). It is worth noting that in the first 5 years after the fire, the DI still showed an upward trend in burn severity (*Slope* = 0.19, 0.40, 0.48), and this dropped significantly after 5 years ($p < 0.001$) (Figure 5b). The reason for this was that in the burned area, reforestation activities were carried out alongside deforestation activities in the first 5 years, and the disturbances were continuously strengthened.

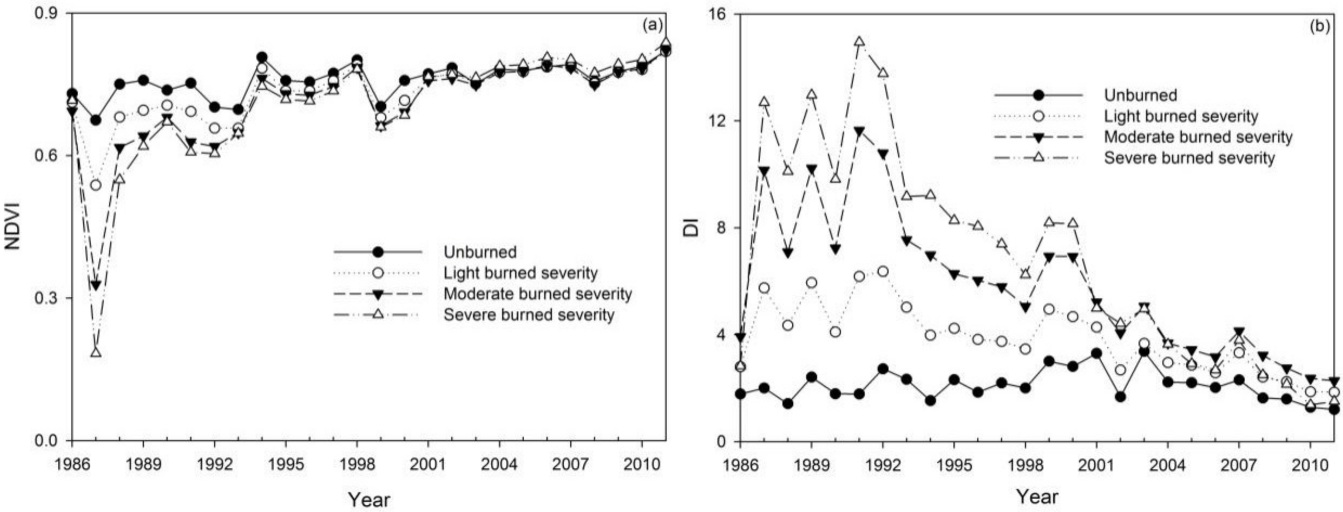

Figure 5. Yearly NDVI (**a**) and DI (**b**) trends with different burn severity classes.

3.2. Comparison of Forest Remote Sensing Index with Different Restoration Methods

Comparing the trends of the NDVI and DI using two different restoration methods, the results showed that with different restoration methods, the NDVI decreased to 0.35 and 0.19, respectively, in the year of fire, but the values recovered quickly after the fire, and recovered to 99% and 98% of the pre-fire level, respectively, in the third year (Figure 6). There were significant differences between the area that underwent artificial recovery and the unburned area in the three periods ($p < 0.05$), while there were no obvious differences between the area that underwent natural recovery and the unburned area (Figure 6a). Compared to the NDVI ($F = 18.06$, $p < 0.001$), the DI showed more sensitivity to these two restoration methods ($F = 37.66$, $p < 0.001$). There were obvious differences between the areas that underwent artificial recovery and natural recovery and the unburned area in the three periods ($p < 0.05$), but the differences between the area that underwent natural recovery, and the unburned area were even smaller (Figure 6b). With different restoration methods, the DI rose to 9.61 and 14.20, respectively, in the year of fire. The artificial restoration methods continued to increase the DI after the fire (*Slope* = 0.84), reaching a peak of 18.65 five years later and then showing a significant downward trend ($p < 0.001$) (Figure 6b). The reason for this could be that during artificial restoration activities, felling took place at the same time. The natural method of restoration exhibited better DI values than the artificial method, and the DI continued to decrease after the fire (Figure 6b). Overall, the NDVI and DI values recovered faster via the natural restoration method.

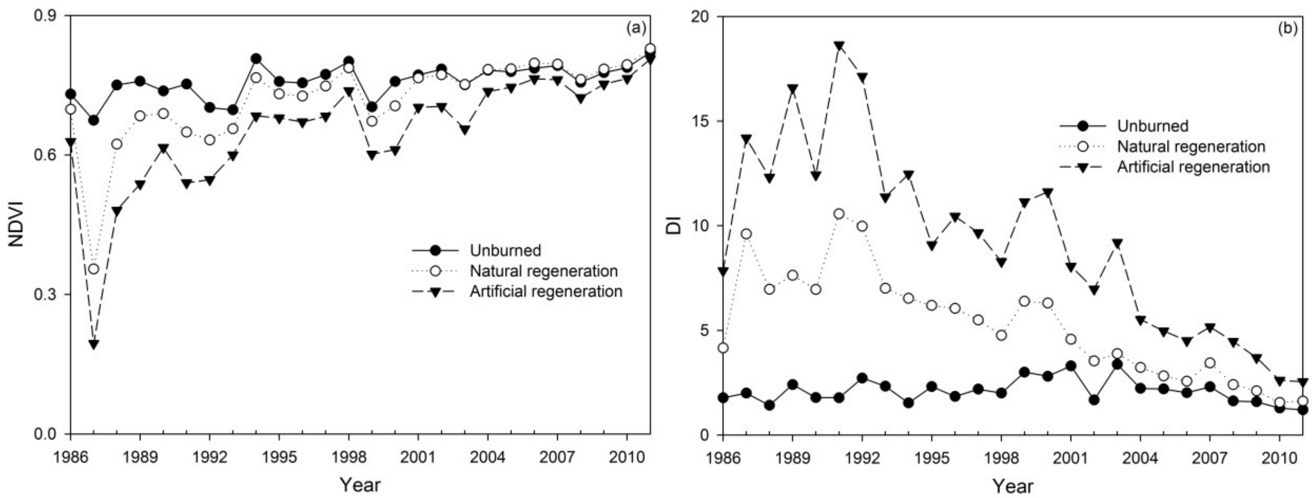

Figure 6. Yearly NDVI (**a**) and DI (**b**) trends with different forest restoration methods.

3.3. Comparison of 2020 Forest Inventory Parameters of Different Burn Severities and Restoration Methods

Thirty-three years after the fire, the forest inventory showed that the average height of trees in the naturally restored area was 10.79 m, the average DBH was 9.88 cm, and both height and DBH decreased as the burn severity increased. However, the canopy density recovered to an average of 0.55 (Table 3). In the artificially restored area, the average height of trees was 9.70 m, and the average DBH was 8.78 cm. There were no regular changes in the height and DBH of trees in areas with different burn severities because of the deforestation activities that took place during the restoration period. However, the canopy density also recovered to 0.56 on average (Table 3). Overall, in the naturally restored area, the average DBH and height values were obviously larger than those in the artificially restored area, while there was little difference in the canopy density in both areas. In terms of the burn severity, in the light severity area, the average DBH and height values in the naturally restored area were larger than those in the artificially restored area. However, in the moderate and severe severity areas, the average DBH and height values were larger in the artificially restored area. In areas with different burn severities, there was also little difference in the canopy density (Table 3). The results regarding canopy density were consistent with the little difference observed in the NDVI or DI values under different burn severity conditions and using different restoration methods after 2011 (Figures 5 and 6).

Table 3. The statistics and comparison of forest parameters with different burn severities and forest restoration methods.

Type	Parameter	Unburned	Burned			Average
			Light Severity	Moderate Severity	Severe Severity	
Natural regeneration	Tree high/m	13.71	12.33	9.73	9.21	10.79
	Diameter at Breast Height/cm	13.55	11.99	8.75	7.7	9.88
	Canopy density	0.57	0.54	0.5	0.57	0.55
Artificial regeneration	Tree high/m	11.7	9.66	10.01	9.82	9.70
	Diameter at Breast Height/cm	11.07	8.58	9.15	8.87	8.78
	Canopy density	0.61	0.53	0.55	0.58	0.56

4. Discussion

4.1. Difference in Response of NDVI and DI to Different Burn Severities

Both the NDVI and DI were sensitive to the fire and the degree of burning in the year the fire took place, but there were differences in their responses to the subsequent forest regeneration process. These two indexes displayed obvious changes before and after the fire, and the more severe the level of burning was, the greater the change was. However, the NDVI recovered quickly after the fire, and there was basically no difference in the areas with different burn severities after 5 years, which was consistent with previous studies [42]. The reason for this could be that the black soil in the Greater Hinggan Mountains area is so fertile that although the fire might have affected the soil [43], the melting of frozen soil maintained the soil moisture and allowed vegetation such as herbs and shrubs to recover rapidly [44,45]. This was observed in the prompt increase in the NDVI values [46]. However, the inventory showed that 13 years after the fire, the forest canopy level patterns were largely different from the pre-fire period and had negative correlations with the burning intensity [38]. At the same time, the study by Hicke [32] showed that the average recovery period of a forest's net primary production (NPP) in North American coniferous forests was 9 years on average. Therefore, the NDVI could not be used to describe the whole continuous restoration process of arborous layers with different burn severities.

The DI could not only describe the whole dynamic recovery process of the forest, but it also displayed obvious distinctions between different burn severities within 20 years after the fire. In addition, the DI could also reflect the influence of felling activities, which means that the DI had a stronger response capability to disturbances such as forest fires, felling activities, and forest regeneration [1,13,29]. The DI combines three Tasseled-Cap components, among which, the wetness component contains shortwave infrared information, which is very important for the evaluation of forest structure changes and is more suitable for the monitoring of forest canopy replacement disturbances [1,47,48]. The brightness and greenness components also have good applicability to the monitoring of clear-cutting disturbances [49]. Compared with the NDVI, which is based on a simple spectrum combination, the DI has a stronger response to the dynamic vegetation restoration of various burn severities and felling activities [28].

4.2. Difference in Response of NDVI and DI to Different Restoration Methods

Both of the remote sensing indices showed that natural restoration was better than artificial restoration. Coniferous species such as *Larix gmelinii* and *Pinus sylvestris* were mainly replanted in the artificial restoration area. Many broad-leaved species such as *Betula platyphylla* and *Populus davidiana* and other herbs and shrubs sprouted first in the naturally restored area. In particular, the DI also showed that logging activities during the process of artificial restoration might have led to the further enhancement of disturbances. Therefore, whether it was judged by the speed of canopy restoration or the total vegetation recovery, the natural restoration method was faster than the artificial method. The field survey indicated that there were only coniferous species of *Larix gmelinii* and *Pinus sylvestris* in the forest area under artificial regeneration. In the natural regeneration area, there were both coniferous species (*Larix gmelinii* and *Pinus sylvestris*) and broad-leaved species (*Betula platyphylla* and *Populus davidiana*), and the latter achieved complete dominance. The previous study also showed that naturally restored forests had the highest canopy vertical density and comparatively more abundant species [2]. Even so, artificial regeneration shortened the succession cycle from broad-leaved forests to coniferous forests [38,50]. In addition, under artificial regeneration, coniferous species might regrow significantly faster than those under natural regeneration [2], especially in moderately and severely burned areas.

Compared with the NDVI, the DI was more suitable for use in monitoring post-fire forest dynamics caused by different restoration methods. The DI was more sensitive and could track different disturbance signals for longer. On the one hand, the DI includes more bands than the NDVI. It combines three Tasseled-Cap components, which are very important in the evaluation of forest structure changes and are more suitable for the monitoring of forest canopy replacement disturbance [1,47,48]. On the other hand, the NDVI uses nonlinear stretching to enhance the reflectance contrast of near-infrared and red light, and it has low sensitivity to high vegetation-covered areas and detection in long time series [2].

4.3. Difference in Restoration Effect of Various Burn Severities and Restoration Methods

According to both forest inventory data and two remote sensing indexes, the burn severity was a very important factor that affected the restoration process and results [51,52]. On the one hand, the differences in the amount and quality of residual bodies were caused by the burn severity. The heavier the fire, the fewer the standing trees that remained, the longer the time needed to recover to the previous level, and the younger the average forest age. On the other hand, the burn severity had various effects on the soil's physicochemical properties and germplasm sources. The heavier the fire, the more soil organic matter and water that was lost [43], the fewer the seeds that survived on the surface and in the soil, and the longer the time needed to recover to the previous canopy status and productivity. However, other research results showed that fire had an insignificant impact on the soil seed bank composition and restoration potential of a plant species from seeds [53,54]. The understory herb and shrub communities have the ability to form a fire-resistant and viable soil seed bank. Meanwhile, the black soil in the Greater Hinggan Mountains area was fertile, and the melting of frozen soil also maintained the soil moisture and allowed vegetation such as herbs and shrubs to recover rapidly [44,45].

Judging from the two remote sensing indexes, and with the support of forest inventory results, we found that the average DBH and height values were larger in the naturally restored area, and the natural restoration method was faster than the artificial restoration method. However, the restoration effect was different under various degrees of burn severity. In the moderately and severely burned areas, artificial restoration achieved better results than natural restoration. Firstly, the burn severity was a direct factor: in severely and moderately burned areas, the artificial method was preferred, while in lightly burned areas, the natural method was implemented [38]. The average burn severities were different using these two methods. Secondly, deforestation influenced the restoration process. Artificial restoration areas are usually more convenient to reach and more accessible than natural areas. In the early stage of the artificial restoration activities, large-diameter timber was being cut down in both the burned area and unburned forest, which led to lower average values of DBH and height. However, the natural restoration area, which was inconvenient to access, was less affected by logging activities. Thirdly, the recovery of the community structure was an important factor. Previous studies showed that natural restoration was more effective in terms of canopy density alone, but in terms of tree species composition, artificial restoration shortened the succession cycle from broad-leaved forests to coniferous forests [38,50]. In addition, the restoration effect was also influenced by site conditions, etc. [55,56].

4.4. Mechanism of NDVI and DI Indicating the Differences in Reforestation Activities

In essence, the different responses of the NDVI and DI to the forest's post-fire regeneration process were due to their different abilities to respond to horizontal and vertical forest structure changes. There were differences between the NDVI and DI on the spectral response characteristic curves of non-vegetation cover, herbs, shrubs, trees, and their combinations. The NDVI quantifies vegetation coverage by using the difference between the strong reflection of vegetation leaves on the near-infrared band and the strong absorption of the red band, while there is basically no difference between the two bands in an area without vegetation cover. Therefore, the NDVI is very sensitive to changes in vegetation cover, especially under conditions of no vegetation cover or low vegetation cover. In 1987, a major portion of the forests, including herbs, shrubs, and trees, were burnt down. Large unvegetated or sparse vegetated areas appeared. The more severe the fire was, the larger the unvegetated or sparse vegetated areas and the lower the vegetation cover was. The NDVI value dropped dramatically. That is to say, the more serious the damage was, the lower the NDVI value was. Vegetation started to recover after the fire. Due to the soil seed banks of herbs and shrubs, these types of vegetation were least affected by the fire [53,54] and were more likely to rely on rhizoid germination [57]; herbs and shrubs preferentially recovered according to different fire damage degrees and recovery methods. Although trees recovered slowly under natural restoration conditions, the total vegetation coverage recovered quickly, and the NDVI value increased rapidly. Meanwhile, in the artificial restoration process, the selective felling of large-diameter trees could have affected the canopy density. However, the replanting of coniferous species such as *Larix gmelini* and *Pinus sylvestris* increased the vegetation coverage. Therefore, the total vegetation cover had little influence, and the NDVI increased quickly as well. Several years later, with the recovery of canopy density, the NDVI increased slowly. Because the NDVI uses nonlinear stretching to enhance the reflectance contrast of near-infrared and red light, it has low sensitivity to high vegetation-covered areas. Therefore, when forests were in the successional stage, from shrubs to trees, the vegetation coverage had already recovered, and there was little difference in the NDVI between various burn severities and restoration methods. This was also probably due to the fact that only two bands were used in the acquisition of the NDVI, making it relatively insensitive to post-fire forest recovery detection in the long time series [2].

Tasseled-Cap transformation reduces the Landsat-5 TM reflectance bands to three orthogonal indices called brightness, greenness, and wetness. The DI is a combination of the three Tasseled-Cap indices. The DI quantifies changes in a forest canopy by the difference between the disturbed stand and the average condition of the undisturbed stand around it. It is more sensitive to changes in a tree canopy [1,58]. When the fire occurred, the brightness value increased quickly, while the greenness and wetness values decreased rapidly. The heavier the damage of the fire was, the more these three indexes changed and the higher the DI value. In the early stage of forest recovery, the selective felling of large-diameter trees reduced the canopy density, which made the DI value increase. When coniferous species were planted and naturally regenerating broad-leaved species grew, the DI value started to decrease. Compared with open forests, the DI was more sensitive to disturbances in dense forests. The lower the succession rate of a forest, such as a boreal conifer forest, the longer the disturbance signal will last in the DI [1].

4.5. Limitations and Caveats

NDVI is sensitive to soil background noise and is difficult to interpret when the vegetation cover is low. Studies have shown that with the same vegetation coverage, the soil with dark color and low reflection rate illustrates a higher NDVI value than the soil with light color and high reflection rate [22,59,60]. Meanwhile, with the same vegetation coverage, the NDVI value is higher in moist soil background than that in dry soil background [61]. The reason is that the reflection rate of the soil becomes lower when there are more organics, iron oxide, or higher moisture content, especially in the band of THE visible light spectrum [62]. Within TM data, soil reflectance characteristics are distributed in a plane defined by wetness as well as brightness [61,63]. Therefore, normalization to minimize soil-related influences on vegetation indices should be based on the more expanded soil plane information [64]. On the other hand, as the vegetation canopy closes, the NDVI saturates and cannot differentiate the variation in vegetation cover [22,23]. The NDVI quantifies the vegetation coverage by using the reflectance difference of vegetation leaves between the near-infrared band and the red band. The major factors controlling vegetation reflectance are the chlorophyll present in the leaves, the structure of the leaf, and the moisture contained in the leaves [65]. Research shows that NDVI is easier to reach saturation with the change in vegetation water content [66]. Though NDVI has great potential and broad usage, it is not a perfect global vegetation index to monitor some special vegetation dynamic characteristics. However, DI provides opportunities to better understand the dynamics of spectral variation across landscapes in relation to heterogeneous soil and vegetation components than NDVI. Wetness and brightness axes provide information not only relevant to soil background characteristics but also to vegetation cover [61].

When using remote sensing image features to analyze canopy restoration results, the time period of the images is an important factor that needs to be taken into consideration. Based on previous studies, after 20 years of recovery in a burned area, it is difficult to observe differences in canopy restoration using the remote sensing index [36–38,45]. The results of our forest inventory in 2020 also showed that there was little difference in forest canopy density under different conditions. The results regarding canopy density were consistent with the little difference observed in the NDVI or DI values under different burn severity conditions and using different restoration methods after 2011. Therefore, in this study, the initial growth stages of trees were selected to represent their growth condition, and remote sensing images from 2011 and onwards were not extracted and analyzed. Since NDVI and DI could only be used as a relative description of the overall conditions of forest ecosystems with no corresponding parameters that could be measured by devices, it was difficult to directly compare the results with field survey data. Additionally, as there were already 36 years after the "5.6 Fire", and we had not collected forest attributes covering such a long period, the ground-based validation synchronized with the time series images appeared impossible. Therefore, instead of directly comparing the forest inventory data with the two remote sensing indexes, we intended to use the inventory data of 2020 to indirectly analyze and verify whether the canopy recovery in the early stage would affect the final productivity.

Natural restoration means that the generation completely depends on seed trees without any human measures, while artificial restoration refers to directly planting young coniferous seedlings (*Larix gmelinii* or *Pinus sylvestris*). In severely and moderately burned areas, the artificial method was preferred, while in lightly burned areas, the natural method was implemented [38]. Artificial restoration areas are usually more convenient to reach and more accessible than natural areas. In the early stage of the artificial restoration activities, large-diameter timber was being cut down in both the burned area and the unburned forest. However, the natural restoration area, which was inconvenient to access, was less affected by logging activities.

5. Conclusions

In this study, we extracted two indexes, the NDVI and DI, based on long-time-series remote sensing data. Combined with forest inventory data, the results of dynamic vegetation restoration before and after the fire showed that both indexes were sensitive to the burn severity and restoration methods but reacted differently to the whole recovery process. In 1987, the NDVI values dropped dramatically while the DI values rapidly increased. The NDVI values returned to the previous level shortly after the fire. Therefore, in the later monitoring period, differences between the various burn severities and restoration methods could not be reflected by the NDVI but could be by the DI. Additionally, the DI was also able to reflect deforestation activities during restoration. Therefore, in comparison with the NDVI, the DI more effectively reflected various burn severities, restoration methods, and felling activities in the restoration process.

Burn severity and restoration methods had essential influences on the forest restoration process. After the fire and during the whole process, the rate of change and recovery times in the NDVI and DI were evidently positively correlated with the burn severity. Forest inventory data 33 years after the fire showed that the average DBH and height values in the naturally restored area decreased as the burn severity increased. Both the NDVI and DI results showed that vegetation recovered faster and better under the natural restoration method. However, the results were also influenced by other factors.

Author Contributions: Conceptualization, G.Z. and E.X.; methodology, G.Z. and E.X.; validation, G.Z., E.X. and X.Y.; formal analysis, G.Z. and X.Y.; investigation, G.Z., E.X. and Y.G.; resources, G.Z. and X.Y.; data curation, G.Z., E.X. and X.Y.; writing—original draft, G.Z. and X.Y.; writing—review and editing, E.X. and K.Z.; supervision, G.Z. and X.Y.; project administration, G.Z.; funding acquisition, G.Z. All authors have read and agreed to the published version of the manuscript.

Funding: This research was funded by the Monitoring and Assessment of the Socio-economic Impacts of China's Key Forestry Programs, grant number 2130237-180902.

Data Availability Statement: The data presented in this study are available upon request from the first author.

Acknowledgments: The authors are grateful to Jing Gao for her help in the revision and polishing of English expressions.

Conflicts of Interest: The authors declare no conflict of interest.

References

1. Healey, S.P.; Cohen, W.B.; Zhiqiang, Y.; Krankina, O.N. Comparison of Tasseled Cap-based Landsat data structures for use in forest disturbance detection. *Remote Sens. Environ.* **2005**, *97*, 301–310. [CrossRef]
2. Chen, W.; Moriya, K.; Sakai, T.; Koyama, L.; Cao, C. Monitoring of post-fire forest recovery under different restoration modes based on time series Landsat data. *Eur. J. Remote Sens.* **2014**, *47*, 153–168. [CrossRef]
3. Walker, X.J.; Baltzer, J.L.; Cumming, S.G.; Day, N.J.; Ebert, C.; Goetz, S.; Johnstone, J.F.; Potter, S.; Rogers, B.M.; Schuur, E.A.G.; et al. Increasing wildfires threaten historic carbon sink of boreal forest soils. *Nature* **2019**, *572*, 520–523. [CrossRef] [PubMed]
4. Kelly, R.; Chipman, M.L.; Higuera, P.E.; Stefanova, I.; Brubaker, L.B.; Hu, F.S. Recent burning of boreal forests exceeds fire regime limits of the past 10,000 years. *Proc. Natl. Acad. Sci. USA* **2013**, *110*, 13055–13060. [CrossRef] [PubMed]
5. Stocks, B.J.; Fosberg, M.A.; Lynham, T.J.; Mearns, L.; Wotton, B.M.; Yang, Q.; Jin, J.Z.; Lawrence, K.; Hartley, G.R.; Mason, J.A.; et al. Climate Change and Forest Fire Potential in Russian and Canadian Boreal Forests. *Clim. Chang.* **1998**, *38*, 1–13. [CrossRef]
6. Seidl, R.; Thom, D.; Kautz, M.; Martin-Benito, D.; Peltoniemi, M.; Vacchiano, G.; Wild, J.; Ascoli, D.; Petr, M.; Honkaniemi, J.; et al. Forest disturbances under climate change. *Nat. Clim. Chang.* **2017**, *7*, 395–402. [CrossRef]
7. Dixon, R.K.; Solomon, A.M.; Brown, S.; Houghton, R.A.; Trexier, M.C.; Wisniewski, J. Carbon pools and flux of global forest ecosystems. *Science* **1994**, *263*, 185–190. [CrossRef]
8. Seiler, W.; Crutzen, P.J. Estimates of gross and net fluxes of carbon between the biosphere and the atmosphere from biomass burning. *Clim. Chang.* **1980**, *2*, 207–247. [CrossRef]
9. Goward, S.N.; Masek, J.G.; Cohen, W.; Moisen, G.; Collatz, G.J.; Healey, S.; Houghton, R.A.; Huang, C.; Kennedy, R.; Law, B. Forest Disturbance and North American Carbon Flux. *Eos Trans. Am. Geophys. Union* **2008**, *89*, 105–116. [CrossRef]
10. Fang, J.; Chen, A.; Peng, C.; Zhao, S.; Ci, L. Changes in forest biomass carbon storage in China between 1949 and 1998. *Science* **2001**, *292*, 2320–2322. [CrossRef]
11. Malhi, Y.; Phillips, O.L.; Lloyd, J.; Baker, T.; Wright, J.; Almeida, S.; Arroyo, L.; Frederiksen, T.; Grace, J.; Higuchi, N. An international network to monitor the structure, composition and dynamics of Amazonian forests (RAINFOR). *J. Veg. Sci.* **2002**, *13*, 439–450. [CrossRef]
12. Loveland, T.R.; Merchant, J.W.; Ohlen, D.O.; Brown, J.F. Development of a land-cover characteristics database for the conterminous U.S. *Photogramm. Eng. Remote Sens.* **1991**, *57*, 1453–1463.
13. Li, L.; Shen, R.; Li, X.; Guo, J. Comparison of Forest Disturbance Indices based on MODIS Time-Series Data. *Remote Sens. Technol. Appl.* **2016**, *31*, 1083–1090.
14. Li, R.R.; Kaufman, Y.J.; Wei, M.H.; Salmon, J.M.; Gao, B.C. A technique for detecting burn scars using MODIS data. *IEEE Trans. Geosci. Remote Sens.* **2004**, *42*, 1300–1308.
15. Wu, L.; Shen, R.; Li, X.; Yang, H. Evaluating Different Remote Sensing Indexes for Forest Burn Scars Extraction. *Remote Sens. Technol. Appl.* **2014**, *29*, 567–574.
16. Röder, A.; Joachim, H.; Beatriz, D.; Antonio, A.J.; Ramon, V. Using long time series of Landsat data to monitor fire events and post-fire dynamics and identify driving factors. A case study in the Ayora region (eastern Spain). *Remote Sens. Environ.* **2008**, *112*, 259–273. [CrossRef]
17. Yang, C.; Shen, R.; Yu, D.; Liu, R.; Chen, J. Forest disturbance monitoring based on the time-series trajectory of remote sensing index. *J. Remote Sens.* **2013**, *17*, 1246–1263.
18. Huang, C.; Goward, S.N.; Masek, J.G.; Thomas, N.; Zhu, Z.; Vogelmann, J.E. An automated approach for reconstructing recent forest disturbance history using dense Landsat time series stacks. *Remote Sens. Environ.* **2010**, *114*, 183–198. [CrossRef]
19. Jin, S.; Sader, S.A. Comparison of time series tasseled cap wetness and the normalized difference moisture index in detecting forest disturbances. *Remote Sens. Environ.* **2005**, *94*, 364–372. [CrossRef]
20. Sellers, P.J.; Berry, J.A.; Collatz, G.J.; Field, C.B.; Hall, F.G. Canopy reflectance, photosynthesis, and transpiration. III. A reanalysis using improved leaf models and a new canopy integration scheme. *Remote Sens. Environ.* **1992**, *42*, 187–216. [CrossRef]
21. Jin, S.; Sader, S.A. MODIS time-series imagery for forest disturbance detection and quantification of patch size effects. *Remote Sens. Environ.* **2005**, *99*, 462–470. [CrossRef]
22. Huete, A.R. A soil-adjusted vegetation index (SAVI). *Remote Sens. Environ.* **1988**, *25*, 295–309. [CrossRef]
23. Turner, D.P.; Cohen, W.B.; Kennedy, R.E.; Fassnacht, K.S.; Briggs, J.M. Relationships between Leaf Area Index and Landsat TM Spectral Vegetation Indices across Three Temperate Zone Sites. *Remote Sens. Environ.* **1999**, *70*, 52–68. [CrossRef]
24. Key, C.H.; Benson, N.C. Landscape Assessment: Ground measure of severity, the Composite Burn Index; and Remote sensing of severity, the Normalized Burn Ratio. In *FIREMON: Fire Effects Monitoring and Inventory System*; Lutes, D.C., Keane, R.E., Caratti, J.F., Key, C.H., Benson, N.C., Sutherland, S., Gangi, L.J., Eds.; USDA Forest Service, Rocky Mountain Research Station: Ogden, UT, USA, 2006; LA 1–51.

25. García, M.J.L.; Caselles, V. Mapping burns and natural reforestation using thematic Mapper data. *Geocarto Int.* **1991**, *6*, 31–37. [CrossRef]
26. Hilker, T.; Wulder, M.A.; Coops, N.C.; Linke, J.; McDermid, G.; Masek, J.G.; Gao, F.; White, J.C. A new data fusion model for high spatial- and temporal-resolution mapping of forest disturbance based on Landsat and MODIS. *Remote Sens. Environ.* **2009**, *113*, 1613–1627. [CrossRef]
27. DeRose, R.J.; Long, J.N.; Ramsey, R.D. Combining dendrochronological data and the disturbance index to assess Engelmann spruce mortality caused by a spruce beetle outbreak in southern Utah, USA. *Remote Sens. Environ.* **2011**, *115*, 2342–2349. [CrossRef]
28. Masek, J.G.; Huang, C.; Wolfe, R.; Cohen, W.; Hall, F.; Kutler, J.; Nelson, P. North American forest disturbance mapped from a decadal Landsat record. *Remote Sens. Environ.* **2008**, *112*, 2914–2926. [CrossRef]
29. Coops, N.C.; Wulder, M.A.; Iwanicka, D. Large area monitoring with a MODIS-based Disturbance Index (DI) sensitive to annual and seasonal variations. *Remote Sens. Environ.* **2009**, *113*, 1250–1261. [CrossRef]
30. DaSilva, M.D.; Bruce, D.; Hesp, P.A.; Miot da Silva, G. A New Application of the Disturbance Index for Fire Severity in Coastal Dunes. *Remote Sens.* **2021**, *13*, 4739. [CrossRef]
31. Wang, J.; Feng, L.; Palmer, P.I.; Liu, Y.; Fang, S.; Bösch, H.; O'Dell, C.W.; Tang, X.; Yang, D.; Liu, L.; et al. Large Chinese l and carbon sink estimated from atmospheric carbon dioxide data. *Nature* **2020**, *586*, 720–723. [CrossRef]
32. Hicke, J.A.; Asner, G.P.; Kasischke, E.S.; French, N.H.F.; Randerson, J.T.; James Collatz, G.; Stocks, B.J.; Tucker, C.J.; Los, S.O.; Field, C.B. Postfire response of North American boreal forest net primary productivity analyzed with satellite observations. *Glob. Chang. Biol.* **2003**, *9*, 1145–1157. [CrossRef]
33. Bunn, A.G.; Goetz, S.J.; Fiske, G.J. Observed and predicted responses of plant growth to climate across Canada. *Geophys. Res. Lett.* **2005**, *32*, L16710. [CrossRef]
34. Goetz, S.J.; Bunn, A.G.; Fiske, G.J.; Houghton, R.A. Satellite-observed photosynthetic trends across boreal North America associated with climate and fire disturbance. *Proc. Natl. Acad. Sci. USA* **2005**, *102*, 13521–13525. [CrossRef] [PubMed]
35. Huang, W.; Hu, Y.; Chang, Y.; Liu, M.; Li, Y.; Ren, B.; Shi, S. Effects of Fire Severity and Topography on Soil Black Carbon Accumulation in Boreal Forest of Northeast China. *Forests* **2018**, *9*, 408. [CrossRef]
36. Huang, H.L.; Cao, Y.; Chen, G.; Xu, L.; Dang, Y.; Singh, R.P.; Bashir, B.; Xie, B.; Lin, X. Remote Sensing Monitoring of Vegetation Dynamic Changes after Fire in the Greater Hinggan Mountain Area: The Algorithm and Application for Eliminating Phenological Impacts. *Remote Sens.* **2020**, *12*, 156. [CrossRef]
37. Chen, X.; Chen, W.; Xu, M. Remote-Sensing Monitoring of Postfire Vegetation Dynamics in the Greater Hinggan Mountain Range Based on Long Time-Series Data: Analysis of the Effects of Six Topographic and Climatic Factors. *Remote Sens.* **2022**, *14*, 2958. [CrossRef]
38. Xie, F.J.; Xiao, D.N.; Li, X.Z.; Wang, X.G.; Dong, S.B. Factorial analysis on forest canopy density restoration in the burned area of northern Great Xing'an Mountains, China. *J. For. Res.* **2005**, *16*, 125–131.
39. Yu, C.; Chen, L.; Li, S.; Tao, J.H.; Su, L. Estimating Biomass Burned Areas from Multispectral Dataset Detected by Multiple-Satellite. *Spectrosc. Spectr. Anal.* **2015**, *35*, 739–745.
40. Huang, C.; Song, K.; Kim, S.; Townshend, J.R.G.; Davis, P.; Masek, J.G.; Goward, S.N. Use of a dark object concept and support vector machines to automate forest cover change analysis. *Remote Sens. Environ.* **2008**, *112*, 970–985. [CrossRef]
41. Crist, E.P. A TM Tasseled Cap equivalent transformation for reflectance factor data. *Remote Sens. Environ.* **1985**, *17*, 301–306. [CrossRef]
42. Qian, D.; Zhang, H.; He, L. Vegetation changes in conflagration area: Case study of Da Hinggan Mountains and Yellowstone National Park burned area. *J. Tianjin Norm. Univ.* **2019**, *39*, 60–68.
43. Verma, S.; Jayakumar, S. Impact of forest fire on physical, chemical and biological properties of soil: A review. *Proc. Int. Acad. Ecol. Environ. Sci.* **2012**, *2*, 168–176.
44. Zhao, F.; Wang, L.; Chen, P.; Shu, L. Review on the Recovery after the Catastrophic Forest Fire in Daxing'anling Mountains. *Forest Resources Management* **2013**, *0*, 125–129.
45. Yang, Y.; Zhang, X.; Xiao, L.; Yang, Y.; Wang, K.; Du, H.; Zhang, J.; Wang, W. Effect of Forest-fire Rehabilitation Time on Plant Diversity in Daxing'an Mountains, Northeastern China. *Bull. Bot. Res.* **2019**, *39*, 514–520.
46. Goetz, S.J.; Fiske, G.J.; Bunn, A.G. Using satellite time-series data sets to analyze fire disturbance and forest recovery across Canada. *Remote Sens. Environ.* **2006**, *101*, 352–365. [CrossRef]
47. Cohen, W.B.; Goward, S.N. Landsat's Role in Ecological Applications of Remote Sensing. *BioScience* **2004**, *54*, 535–545. [CrossRef]
48. Horler, D.N.H.; Ahern, F.J. Forestry information content of Thematic Mapper data. *Int. J. Remote Sens.* **1986**, *7*, 405–428. [CrossRef]
49. Gómez, C.; White, J.C.; Wulder, M.A. Characterizing the state and processes of change in a dynamic forest environment using hierarchical spatio-temporal segmentation. *Remote Sens. Environ.* **2011**, *115*, 1665–1679. [CrossRef]
50. Wang, X.; Li, X.; Kong, F.; Li, Y.; Shi, B.; Gao, Z. Model of vegetation restoration under natural regeneration and human interference in the burned area of northern Daxinganling. *Chin. J. Ecol.* **2003**, *22*, 30–34.
51. Turner, M.G.; Romme, W.H.; Gardner, R.H.; Hargrove, W.W. Effects of fire size and pattern on early succession in Yellowstone National Park. *Ecol. Monogr.* **1997**, *67*, 411–433. [CrossRef]
52. Reyes, O.; Casal, M. Regeneration models and plant regenerative types related to the intensity of fire in Atlantic shrubland and woodland species. *J. Veg. Sci.* **2008**, *19*, 575–583. [CrossRef]

53. Konsam, B.; Phartyal, S.S.; Todaria, N.P. Impact of forest fire on soil seed bank composition in Himalayan Chir pine forest. *J. Plant Ecol.* **2019**, *13*, 177–184. [CrossRef]
54. Daibes, L.F.; Zupo, T.; Silveira, F.; Fidelis, A. A field perspective on effects of fire and temperature fluctuation on Cerrado legume seeds. *Seed Sci. Res.* **2017**, *27*, 74–83. [CrossRef]
55. Shen, Z.; Zhang, X.; Jin, Y. Gradient analysis of the influence of mountain topography on vegetation pattern. *Acta Phytoecol. Sin.* **2000**, *24*, 430–435.
56. Kong, F.; Li, X.; Yin, H.; Wang, X.; Xie, F. Gradient analysis on the influence of terrain on the forest landscape pattern in the burned blanks of the north slope of Mt.Daxing'anling. *Acta Ecol. Sin.* **2004**, *24*, 1863–1870.
57. Blodgett, H.; Hart-Fredeluces, G.; Stanislaw, M. *Annual Burning Decreases Seed Density in the Upper Soil Layers of the Seed Bank*; Biology Department, Grinnell College: Grinnell, IA, USA, 2012.
58. Hais, M.; Jonášová, M.; Langhammer, J.; Kučera, T. Comparison of two types of forest disturbance using multitemporal Landsat TM/ETM+ imagery and field vegetation data. *Remote Sens. Environ.* **2009**, *113*, 835–845. [CrossRef]
59. Heilman, J.L.; Boyd, W.E. Soil background effects on the spectral response of a three-component rangeland scene. *Remote Sens. Environ.* **1986**, *19*, 127–137. [CrossRef]
60. Huete, A.R.; Jackson, R.D. Suitability of spectral indices for evaluating vegetation characteristics on arid rangelands. *Remote Sens. Environ.* **1987**, *23*, 213–232. [CrossRef]
61. Todd, S.W.; Hoffer, R.M. Responses of Spectral Indices to Variations in Vegetation Cover and Soil Background. *Photogramm. Eng. Remote Sens.* **1998**, *64*, 915–921.
62. Hoffer, R.M. Biological and Physical Considerations in Applying Computer-aided Analysis Techniques to Sensor Data. In *Remote Sensing: The Quantitative Approach*; Swain, P.H., Davis, S.M., Eds.; McGraw-Hill: New York, NY, USA, 1978.
63. Huete, A.R.; Jackson, R.D.; Post, D.F. Spectral response of a plant canopy with different soil backgrounds. *Remote Sens. Environ.* **1985**, *17*, 37–53. [CrossRef]
64. Huete, A.R.; Tucker, C.J. Investigation of soil influences in AVHRR red and near-infrared vegetation index imagery. *Int. J. Remote Sens.* **1991**, *12*, 1223–1242. [CrossRef]
65. Redowan, M.; Kanan, A.H. Potentials and Limitations of NDVI and other Vegetation Indices (VIS) for Monitoring Vegetation Parameters from Remotely Sensed Data. *Bangladesh Res. Publ. J.* **2012**, *7*, 291–299.
66. Jackson, T.J.; Chen, D.; Cosh, M.; Li, F.; Anderson, M.; Walthall, C.; Doriaswamy, P.; Hunt, E.R. Vegetation water content mapping using Landsat data derived normalized difference water index for corn and soybeans. *Remote Sens. Environ.* **2004**, *92*, 475–482. [CrossRef]